Molecular Dynamics Simulations of Human LRH-1: The Impact of Ligand Binding in a Constitutively Active Nuclear Receptor[†]

Sofia Burendahl, Eckardt Treuter, and Lennart Nilsson*

Department of Biosciences and Nutrition, Karolinska Institutet, SE-141 57 Huddinge, Sweden

Received December 21, 2007; Revised Manuscript Received March 18, 2008

ABSTRACT: The liver receptor homologue 1 (LRH-1 (NR5A2)) belongs to the orphan nuclear receptor family, indicating that initially no ligand was known. Although recent studies have shown that ligand binding can be obtained, the biological relevance remains elusive. Here, we modify the observed X-ray ligand into a biologically more significant phospholipid (phosphatidylserine, PS) present in human, to study, by molecular dynamics (MD) simulations, the impact of the ligand on the receptor and the interaction with different cofactor peptides. Furthermore, we characterize the interactions between receptor and the cofactor peptides of DAX-1 (NR0B1), Prox1 and SHP LXXLL box 1 and 2 (NR0B2) in terms of specificity. Our MD simulation results show different interaction patterns for the SHP box2 compared to DAX-1, PROX1 and SHP box1. SHP box2 shows specific interactions at its more C-terminal end while the other investigated peptides show specific interactions at several positions but particularly at the +2 site. The peptide +2 side chain interacts with a charged amino acid of the receptor, in hLRH-1 Asp372. Together with the charge clamp residues Arg361 and Glu534, Asp372 forms a triangle shaped charge clamp responsible for peptide orientation and increased affinity. The binding of the PS ligand causes no overall structural changes of the receptor but affects the interactions with cofactor peptides. The cofactor peptides from SHP decrease its interaction with the receptor upon ligand binding while DAX-1 and PROX1 are unchanged or increase. The diverse ligand binding response of the cofactor provides an opportunity for drug design with the possibility to create agonist ligands to modify cofactor interaction.

In the mid-1970s nuclear receptor research entered into a new era (*1*). Steroids were identified as fat soluble molecules; hence they could be transported through a lipid bilayer cell membrane to interact with their target receptor. This result became the platform for the classical model of steroid hormone action, in which the binding of a hormone induces an allosteric change in the receptor, transforming it into a state which is able to bind to DNA and modulate transcription. Further on, the first cloning of a nuclear receptor was performed. This opened for the possibility to understand the nuclear receptor action on a molecular level. It was shown that distinct ligands interact with structurally similar receptors. Nuclear receptors have a conserved modular structure, described in an A−E manner: The A/B domain often holds the ligand independent activation function-1 (AF-1[1]); the C domain contains the highly conserved DNA-binding domain (DBD); the D domain is the flexible hinge region, and the E domain constitutes the ligand binding domain (LBD) including the ligand dependent activation function-2 (AF-2). In the early 1990s the discovery of the retinoid X receptor (*2*) modified the view of hormone signaling, identifying a heteropartner for the receptors. Additionally a new subfamily of NRs was found, the orphan receptors. This group initially lacked natural agonist ligands. In the absence of ligand activation other possible mechanisms were investigated, showing that the mechanism of action of the NRs is more complex than initially suggested. Both the receptor type, post-translational modifications and its location (environment) will affect the individual receptor mechanism. Nuclear receptors constitute one of the largest groups of the transcriptional factors: 48 members have been identified in the human genome and divided into seven subfamilies (NR0−NR6) (*3*). Vertebrate members of the subfamily NR5A including the orphan receptor liver receptor homologue-1 (LRH-1, NR5A2) regulate important steps of development, endocrine homeostasis and metabolism (*4*−*6*). Its closest mammalian homologue is the steroidogenic factor-1 (SF-1, NR5A1), a regulator of development and steroidogenesis.

LRH-1 acts via a non-"classical" regulatory NR mechanism (*7*). Since LRH-1 is an orphan receptor, it does not show a transition between distinct conformations in response to a ligand. Instead other signals, like post-translational modifications, have been shown to affect LRH-1 activity (*8*). Although the LRH-1 regulatory mechanism is nonclassical

[†] This work was supported by the Swedish Research Council.

* Corresponding author: Lennart.Nilsson@biosci.ki.se. Tel: +46-8-6089228. Fax: +46-8-6089290.

[1] Abbreviations: hLRH-1, human liver receptor homologue-1; PS, phosphatidylserine; DBD, DNA binding domain; LBD, ligand binding domain; AF-1, activation function-1; AF-2, activation function-2; NRs, nuclear receptors; SHP, small heterodimer partner; DAX-1, dosage-sensitive sex reversal; DSS, adrenal hypoplasia congenital; AHC, critical region on the X chromosome, gene 1; PROX1, Prospero-related homeobox protein 1; RXR, retinoid X receptor; AR, androgen receptor; VDR, vitamin-D receptor; HNF4, hepatocyte nuclear factor 4; LXR, liver X receptor; ER, estrogen receptor; TR, thyroid-hormone receptor; FXR, farnesoid X receptor; PPAR, peroxisome proliferators-activated receptor; NR0B1, nuclear receptor subfamily 0, group B, member 1; NR0B2, nuclear receptor subfamily 0, group B, member 2; NR5A2, nuclear receptor subfamily 5, group A, member 2.

10.1021/bi7025084 CCC: $40.75
Published on Web 04/15/2008

and other signals than ligand can be utilized, a possible ligand function cannot be excluded (*9*). The available hLRH-1 X-ray structure results demonstrate that the receptor forms an active conformation both with and without a ligand bound to it (*9*−*11*). The bound phosphatidylethanolamine ligand in the X-ray structure is however likely a trace of the X-ray crystal preparation; hence its biological importance can be discussed. Biochemical studies of the ligand binding also indicate that a bound ligand has a dissociation rate constant similar to the rate of the LBD denaturation, thus a bound ligand would not be exchanged during the receptor lifetime (*9*). On the contrary, biochemical and structure biological experiments found that the mouse LRH-1 (sequence identity 89%) had a true ligand independent mechanism where the LBD closes at the lower part, leaving the ligand binding pocket inaccessible for ligands (*10*). These two extremes can be compared to the close homologue hSF-1 (65% sequence identity in LBD) where studies reveal a phospholipid ligand bound and also readily exchanged, indicating that the ligand plays a regulatory role (*12*). Altogether, the ligand binding of hLRH-1 remains elusive. What will happen if the observed ligand in the X-ray structure is modified into a biologically relevant phospholipid ligand present in humans (*13*)? How does the receptor complex, with different cofactor peptides, respond to the presence of a ligand?

The transcriptional activity levels of the NRs can be modified by cofactors which can be regarded as molecular sensors that respond to a cellular context (*8*). The cofactor proteins work as mediators and recruit members of a larger protein complex which can either promote or repress transcription. Cofactors work in a combinatorial way and specific combinations can be found for particular NRs depending on the context. Coactivators bind the receptor and increase transcriptional activity of the target gene by recruitment of the basal transcriptional machinery (*8, 14*). The coactivators interact with the receptor agonist conformation in which AF-2 is available and recognizes an α-helical LXXLL core motif, where L is a leucine and X any amino acid (*8, 15, 16*). The major regulatory effect of LRH-1 is however achieved through the corepressors, which can turn off the constitutively active receptor. The corepressors binding LRH-1 differ from the Class I corepressors (CoR I) in the mechanism of molecular recognition (N-CoR, SMRT). CoR I repressors contain a longer interaction motif (LXX I/H IXXX I/L) (*8*), and they bind to a receptor conformation when the AF-2 surface is not available. The constitutively active LRH-1 conformation excludes the CoR I group from interaction, but allows corepressors that can form interactions with the agonist conformation. This second group of corepressors, here referred to as Class II Corepressors (CoR II), share features with the coactivators. The CoR IIs bind the AF-2 surface of the receptor with a LXXLL-motif. This creates a competition for the AF-2 surface where both coactivators and corepressors can bind. The high resemblance on a molecular basis between the coactivators and corepressors, as well as their interaction with NRs, has been demonstrated with biochemical and stereochemical approaches (*17*). Although the cofactors show a high general similarity, molecular studies have revealed that specificity is obtained on both molecular and tissue levels. Amino acids adjacent to the core motif have been suggested to be important for specificity. Early reports suggested that cofactor peptide C-terminal residues hold the specificity (*18*), while others have proposed residue positions −2, −1 and +6 (numbering the first L in LXXLL as +1) (*18, 19*). Attempts have been made to classify the cofactors into groups according to sequence similarity, which revealed a group with conserved residues at position −2 (serine/threonine) and −1 (hydrophobic amino acid) (*20*). This group of cofactors lacks a charged residue before the LXXLL-core, thus the receptor AF-2 interaction surface does not need the charge clamp to orient the cofactor to the receptor. Additionally it was suggested that this group of cofactors only comprises corepressors, due to the observation that SHP and DAX-1 fit into the group (*20*).

Table 1: Simulated LRH-1 Systems[a]

simulation name	peptide sequence													
SHP box1	A	S	R	P	A	I	**L**	**Y**	**A**	**L**	**L**	S	S	S
SHP box2	A	P	V	P	S	I	**L**	**K**	**K**	**I**	**L**	**L**	E	E
DAX-1	P	R	Q	G	S	I	**L**	**Y**	**S**	**L**	**L**	T	S	S
PROX1	G	E	K	S	N	V	**L**	**R**	**K**	**L**	**L**	K	R	A

[a] Simulations with a ligand present are named with an addition of ps (e.g., SHP box1-ps). The LXXLL motif is indicated by boldface. The peptide amino acid numbering starts with +1 at the first L in the LXXLL motif, and −1 at the amino acid to the left of the LXLLL.

Here, we investigate the interaction between the hLRH-1 and 4 different peptides, each containing 14 amino acids, derived from three relevant corepressors (*21*−*24*): SHP (NR0B2) LXXLL-box1 (SHP box1) available in the X-ray structure of LRH-1 (*9*), the biologically active SHP box2 (SHP box2), DAX-1 (NR0B1) box3 (DAX-1) and PROX1 box1 (PROX1). The corepressor peptides are modeled to the receptor complex, with and without the ligand PS bound to it.

METHODS

Simulations. The modeled LRH-1 complex was based on the coordinates from the Protein Data Bank (*25*) entry 1YUC, including the human LRH-1 (chain A), a phospholipid, a cofactor peptide (SHP) and 140 crystallographic water molecules (*9*). The LRH-1 protein contains 7 titratable histidine residues, of which 6 point to the exterior and one is located at the protein interior. All of the His residues were protonated at the NE2 atom (*26*). Hydrogen atoms were added as previously described (*27*) using the program CHARMM (*28*). Amino acid numbering is set according to hLRH-1, used in the studies of Ortlund et al. (*9*).

The different cofactor peptide sequences of SHP box2, PROX1 and DAX-1 (Table 1) were modeled into the complex by using the backbone coordinates of the peptide in the SHP box1 X-ray structure and the side chains added in an extended conformation. The phospholipid L-α-phosphatidyl-β-oleoyl-γ-palmitoyl-phosphatidylethanolamine (EPH) present in the X-ray structure was modified to phosphatidylserine (PS) by exchanging the headgroup carbon, to a serine (Figure 1). The ligand parameters were picked from the CHARMM protein and lipid parameter files. The complexes were solvated in a 35 Å radius sphere of TIP3P (*29*) water, where all water molecules within 2.8 Å of the solute were removed. With the protein complex and water sphere oriented to the same origin, a water shell around the protein of >5 Å is obtained (Figure 2).

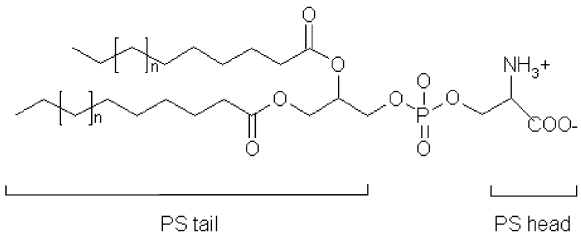

FIGURE 1: PS ligand with serine headgroup and fatty acid tail.

The simulations were performed with stochastic deformable boundary conditions (*28*) in a sphere geometry of 35 Å radius with a friction coefficient $\beta = 50$ ps^{-1} applied to all water oxygens. The potential energy and forces of nonbonded interactions were smoothly shifted to zero at 12 Å, and at 14 Å a nonbonded list generation cutoff was used. The hydrogen and nonbonded list were updated heuristically. The temperature was set to 300 K and allowed to vary in a region of ±5 K. SHAKE (*30*) was used to constrain X−H bonds during the MD simulations, allowing a time step of 2 fs to be used. The structure was relaxed to the CHARMM22 all-atom force field (*26*) by 50 steps of steepest descent minimization and 50 steps of adopted-basis Newton−Raphson minimization, while the α carbons of LRH-1 and peptide were highly restrained (force constant 50.0 kcal/mol/Å^2). The restraints were released and the minimized complexes were simulated for 10 ns and coordinates saved every ps. We did not apply any position restraints during the MD simulation since only small structural changes (backbone rmsd ∼0.5 Å) were observed in the cofactor binding region of the receptor during the first 100 ps of the simulation.

Analysis. All analyses were performed on a merged trajectory where overall rotation and translation were removed based on the LRH-1 minimized coordinates. As a comparative structure for the analysis, the initial minimized structure was used, unless otherwise noted. The analysis was performed on time windows of 1−10 ns.

A hydrogen bond interaction is defined as a connection between a hydrogen and acceptor within 2.4 Å without application of any angular criterion (*31*). The hydrogen bond occupancy is calculated over the 10 ns simulation time, and only hydrogen bonds with occupancies >5% are presented. Hydrogen bond average lifetime was calculated as the total time a given hydrogen bond was present in the simulation divided by the number of hydrogen bonding events. Hydrogen bonds detected at the peptide terminal atoms HT and OT are not considered in the result and discussion although they are presented in Table 2. The atoms HT and OT are used as terminal atoms in our model and thus an artificial construct.

The solvent accessible surface area is calculated with a probe radius of 1.4 Å (*32*).

The root-mean-square fluctuations (rmsf) were calculated for backbone or side chain over the last 5 ns of the simulation. Overall rotation and translation was removed before calculation by least-squares superposition of the backbone atoms on the starting structure. The consistency of the rmsf calculations was investigated by calculating the rmsf over 5 different time windows (1 ns each). The individual data from each 1 ns window compared well with the 5 ns window (data not shown).

RESULTS

Overall Structure. No major changes of the overall LRH-1 structure are observed in any of the 8 different simulated complexes. The secondary structure elements are preserved and are kept in the same positions. This is reflected in the root-mean-square deviation (rmsd) from the starting structure of the LRH-1 backbone alpha carbons, which remains stably at ∼1.5 Å during the whole simulation time (data not shown). A small increase in rmsd is observed for the SHP box1-ps simulation at around 8 ns. This shift is due to a movement of the h1−h3 loop toward h6. The root-mean-square fluctuations (rmsf) of the receptor backbone show larger fluctuations in the loop regions compared to the more ordered secondary structure elements (data now shown). The rmsf does not change significantly due to the introduction of the PS ligand in either of the complexes. Furthermore, the receptor backbone dihedral angles fall in the allowed regions of the Ramachandran plot (data not shown). The α-helix content of the cofactor peptides ranges from 8 residues (SHP box1-ps) to 11 residues (PROX1-ps) (Figure 3a−h). Since this is a relatively short helix, the observed length variation may just be a random end effect. The rmsf of the peptide backbones shows a stable core of about 10 amino acids while the N- and C-terminal ends show larger fluctuations (Figure 4).

Generally, there is only little movement in the tails of the PS ligand and some more in the PS head. In the SHP box1 simulation the ligand head moves in between h7 and h11. The ligand seems to favor a position toward h7 but shifts position between h7 and h11 several times during the simulation. In the SHP box2 simulation the ligand stabilizes toward the h6−h7 loop, while in the DAX-1 simulation the ligand flips between the h1−h3 and h6−h7 loops. An even more flexible positioning is observed in the PROX1 simulation, where the ligand head moves around between the receptor loops h1−h3, h6−h7 and h11−h12. No particular conformation seems to be favored in this simulation. Due to the conformational changes of the PS ligand at the bottom loop region of the receptor, some influences are observed on the receptor structure. Particularly the h1−h3 loop is affected; in the SHP box1-ps simulation the h1−h3 loop shifts from toward h11 (at 3 ns) to the middle and finally toward h6 (at 8 ns). SHP box2-ps shows some displacement of h6, and the DAX-1-ps simulation shows a twist in the h1−h3 loop. In the PROX1-ps simulation both a twist in the h1−h3 loop and some unwinding of h6 N-terminal is observed.

Interactions between the Receptor and Cofactor Peptide. In the hLRH-1 receptor five amino acid participate in cofactor peptide hydrogen bond interactions: Glu358, Arg361, Asp372, Gln379 and Glu534 (Table 2). The charge-clamp residues Arg361 and Glu534 (*16, 33*) are found to interact with the peptide in all simulations apart from SHP box1-ps and SHP box2. In addition to the charge-clamp, Asp372 interacts with all peptide sequences. Asp372 either serves as an extra hydrogen bond interaction site for the peptide or, as in the simulation with SHP box1-ps, takes the Glu534 interaction position in its absence. Asp372 only forms specific hydrogen bond interactions with the peptides, whereas Gln379 acts exclusively as a nonspecific interaction partner for the N-terminal part of the peptide, further stabilizing this region.

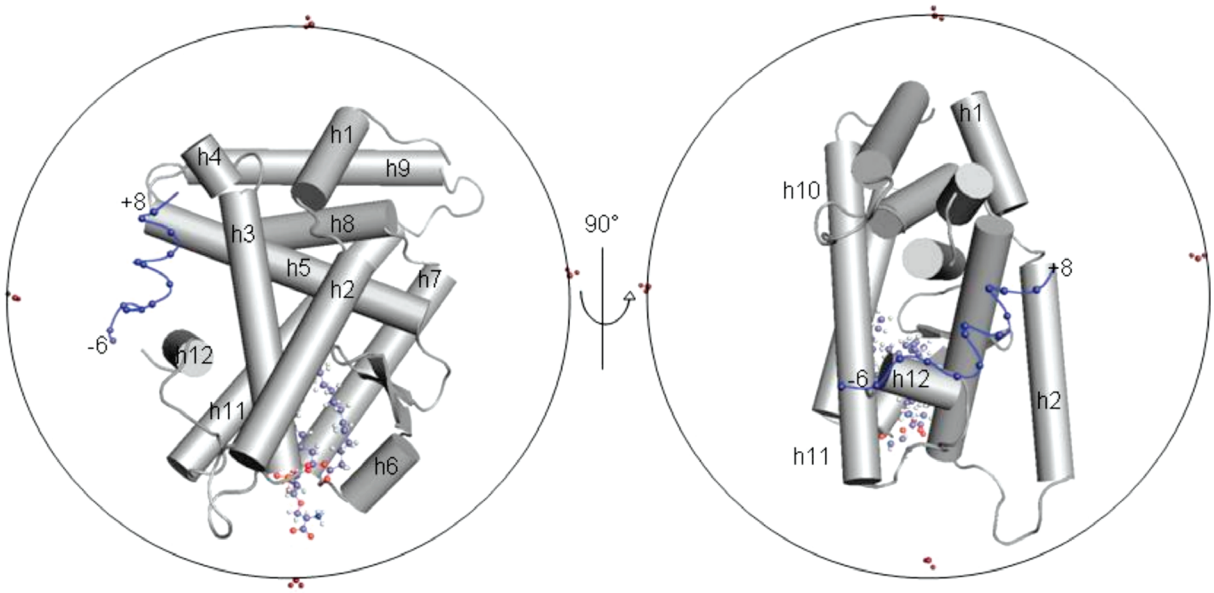

FIGURE 2: Initial conformation of hLRH-1 with cofactor peptide and ligand PS bound to it. The sphere around the complex indicates the outer line of the solvent sphere. The helices of LRH-1 are labeled h1−h12, and the direction of the peptide sequence is indicated with the first (−6) and the last (+8) residue. The ligand PS is shown in balls and sticks. The PS ligand fatty acid tails are covered by the LRH-1 receptor, and the serine headgroup is located at the receptor bottom and solvent exposed.

The specific Glu358 interaction is only observed in the PROX1-ps simulation. The total number of protein residues involved in hydrogen bonds to the peptide varies from 2 (SHP box1-ps) to 5 (PROX1-ps).

The interaction sites of the peptides range from the first residue to the last. In general the interactions from the charge-clamp residues go to the peptide N-terminal and C-terminal regions. In addition the positive side chain of a central residue (+2) interacts with Asp372 in all peptides but not in the simulation SHP box2 although the peptide SHP box2 has a positive lysine at this position.

Cofactor Peptide−hLRH-1 Interaction upon Ligand Binding. In the SHP box1 simulations the total hydrogen bond occupancy and number of interactions involved in hydrogen bonds decrease when PS is introduced to the complex. However, it is mostly the nonspecific interactions that are lost. Two of 3 specific interaction residues are kept in the SHP box1-ps, and the total specific occupancy is unaffected: 149% in SHP box1 and 147% in SHP box1-ps. SHP box2 simulations show the weakest hydrogen bond interactions compared to the other simulated peptides. SHP box2-ps exhibit a lower total hydrogen bond occupancy (SHP box2, 185%; SHP box2-ps, 48%) but additional interactive peptide residues (SHP box2, 2; SHP box2-ps, 4). The specific interactions are kept. Interestingly, the DAX-1 simulations show a various pattern. Here, the total occupancy is decreased with PS (DAX-1, 502%; DAX-1-ps, 281%) as well as the total number of hydrogen bond interactions (DAX-1, 8; DAX-1-ps, 6), but the specific hydrogen bond interactions are increased (DAX-1, 2; DAX-1-ps, 4). In the PROX1 simulations a similar trend is observed. Here the total occupancy slightly decreases with PS (Prox, 639%; PROX1-ps, 568%) but both total and specific interactions are increased (PROX1, 7; PROX1-ps, 10; PROX1, 2, PROX1-ps, 4) as well as the specific occupancy (PROX1, 239%, to PROX1-ps, 457%).

Ligand Binding. The pattern of hydrogen bonds between the receptor and the ligand differs in all simulations (Table 3). However, the receptor amino acids Thr341 (h3), Gln419 and Gly421 (h6−h7 loop), Tyr516 and Lys520 (h11) are frequently observed PS hydrogen bond partners in all complexes. Additional hydrogen bond partners are found in amino acids adjacent to these. The hydrogen bond partners are located in a structural element described to be contacted by the ligand in the overall structural analysis.

LRH-1 Packing. The canonical folding of the secondary structure elements of nuclear receptor is frequently described as completed with the binding of a ligand (*34*). Therefore the receptor packing is often discussed in the context of orphan receptors, since these receptors lack the extra contribution of structural stability obtained from a ligand. In the LRH-1 structure the helix h2 is suggested to contribute to the unliganded receptor stability. We have studied the accessible surface area (ASA) of h2 and the radius of gyration of LRH-1 (Table 4). Comparing the average ASA values of the liganded and empty simulations, both SHP simulations show lower ASA with ligand bound, and the opposite is valid for DAX-1 and Prox 1. However, the differences described are within the standard deviations. The average values of the radius of gyration also differ between the liganded and unliganded simulation, with lower values for the liganded SHP box2 and Prox and higher for SHP box1 and DAX-1. As in the ASA analysis, the variations of the average radius of gyration values are found within the standard deviations.

DISCUSSION

General. The model of the hLRH-1 bound to a peptide sequence and ligand shows a high degree of stability during a 10 ns simulation time. The receptor structure has a low deviation from its original conformation (rmsd), and the residues fluctuate little (rmsf). No abnormal strains are found in the receptor backbone, and the secondary structure elements are preserved. Comparing the analysis of receptor stability (rmsd, rmsf, Ramachandran plot and visual structural

Table 2: Hydrogen Bond Analysis[a]

cofactor peptide aa	receptor aa	occupancy[b] (%)	av time[c] (ps)	cofactor peptide aa	receptor aa	occupancy[b] (%)	av time[c] (ps)
			SHP Box1				
Arg3 sc	**Asp372**	**70 (88)**	**98**	Leu11 bb	Arg361	5 (5)	10
Ala5 bb	Glu534	29 (54)	16	Ser13 bb	Arg361	16 (16)	19
Ile6 bb	Glu534	18 (31)	19	**Ser14 sc**	**Arg362**	**5 (5)**	**140**
Leu7 bb	Glu534	9 (9)	43	Ser14 tm	Arg361	27 (83)	34
Tyr8 sc	**Asp372**	**47 (56)**	**29**	TOTAL		319 (149)	
Leu10 bb	Arg361	48 (55)	97				
			SHP Box1-ps				
Arg3 sc	**Asp372**	**39 (120)**	**64**	Ser13 bb	Arg361	19 (25)	7
Tyr8 sc	**Asp372**	**18 (27)**	**29**	Ser14 tm	Arg361	6 (6)	23
Leu10 bb	Arg361	59 (64)	89	TOTAL		254 (147)	
Leu11 bb	Arg361	18 (18)	21				
			SHP Box2				
Ala1 tm	Asp372	17 (29)	78	**Glu13 sc**	**Arg361**	**48 (116)**	32
Ile10 bb	Arg361	69 (69)	38	TOTAL		185 **(116)**	
			SHP Box2-ps				
Ala1 tm	Asp372	17 (29)	104	Ile10 bb	Arg361	8 (8)	6
Pro2 bb	Gln379	14 (14)	24	**Glu13 sc**	**Arg361**	**12 (19)**	108
Val3 bb	Gln379	7 (7)	55	TOTAL		48 (19)	
			DAX-1				
Arg2 bb	Gln379	66 (66)	24	Leu10 bb	Arg361	53 (92)	111
Arg2 sc	**Glu534**	**58 (197)**	124	Leu11 bb	Arg361	36 (36)	24
Gln3 bb	Gln379	13 (13)	9	Ser13 bb	Arg361	9 (17)	8
Ser5 bb	Glu534	5 (5)	20	Ser14 tm	Arg361	8 (22)	25
Tyr8 sc	**Asp372**	**40 (76)**	23	TOTAL		502 (273)	
			DAX-1-ps				
Arg2 bb	Gln379	8 (8)	30	**Gln3 sc**	**Lys376**	**19 (55)**	29
Arg2 sc	**Glu534**	**12 (21)**	118	**Tyr8 sc**	**Asp372**	**51 (100)**	21
Gln3 bb	Gln379	55 (55)	26	Ser14 tm	Arg361	73 (205)	79
Gln3 sc	**Asp372**	**21 (42)**	20	TOTAL		281 **(218)**	
			PROX1				
Ser4 sc	**Glu534**	**90 (90)**	128	Leu10 bb	Arg361	59 (59)	339
Asn5 bb	Glu534	95 (118)	9	Arg13 bb	Arg361	8 (8)	8
Val6 bb	Glu534	90 (119)	79	Ala14 tm	Arg361	9 (17)	33
Leu7 bb	Glu534	96 (96)	213	TOTAL		639 **(239)**	
Arg8 sc	**Asp372**	**40 (149)**	70				
			PROX1-ps				
Glu2 bb	Gln379	5 (5)	17	Val6 bb	Glu534	8 (8)	19
Lys3 bb	Gln379	7 (7)	15	**Arg8 sc**	**Asp372**	**98 (272)**	612
Lys3 sc	**Asp372**	**18 (47)**	115	Leu11 bb	Arg361	46 (59)	26
Ser4 bb	Gln379	23 (23)	29	**Arg13 sc**	**Glu358**	**17 (52)**	39
Ser4 sc	**Glu534**	**56 (86)**	166	Ala14 tm	Arg361	12 (38)	24
Asn5 bb	Glu534	9 (9)	46	TOTAL		568 **(457)**	

[a] Hydrogen bonds with an occupancy >5% are presented. Specific hydrogen bond interactions (sc) are shown in bold. Peptide numbering starts with 1 from at the N-terminal residue. [b] The maximum occupancy for a single atom pair in % and within parentheses is the sum of occupancies between the residues in %. [c] Average binding time (ps) is presented for the hydrogen bond with the maximum occupancy.

analysis) of the SHP box1 simulation to the other simulations reveals no differences. We can therefore conclude that the docking of the different peptide sequences to the receptor and the insertion of a human ligand were successful. The results also indicate that the receptor can preserve its active agonist conformation while bound to the different peptide sequences and ligand PS.

Specificity of Corepressor Binding. According to our 10 ns simulations the hLRH-1 and peptides SHP box1 and 2, DAX-1 and PROX1, show interactions with several contributing partners. The hydrophobic interface between the peptide leucine residues and receptor surface makes it possible to form a network of van der Waals contacts. The stability of this interaction is reflected in the low rmsf values for the residues involved (Figure 4). In addition to this stable core interaction, polar or charged amino acids adjacent to the LXXLL motif frequently form hydrogen bonds with LRH-1. Hydrogen bonds between the cofactor peptide and receptor can be obtained with different degree of specificity; a hydrogen bond to the peptide backbone can be considered as less specific than a hydrogen bond to the amino acid side chain. In general both specific and nonspecific hydrogen bonds were observed. From the LRH-1, the Gln379 is exclusively involved in nonspecific interactions. Arg361 forms nonspecific interactions in all simulations except SHP box2, and Glu534 forms both types of interactions. Asp372 is almost entirely involved in specific contacts. Residues Arg361, Asp372 and Glu534 seem to be the ones responsible for orienting the cofactor peptide and increase the affinity between the receptor and peptide. Residues Arg361 and Glu534 have previously been reported to form charge-clamp in LRH-1 (*33*). Therefore it is not surprising that these charged residues form hydrogen bonds to the ends of the cofactor peptides. Met375 has been reported as an additional

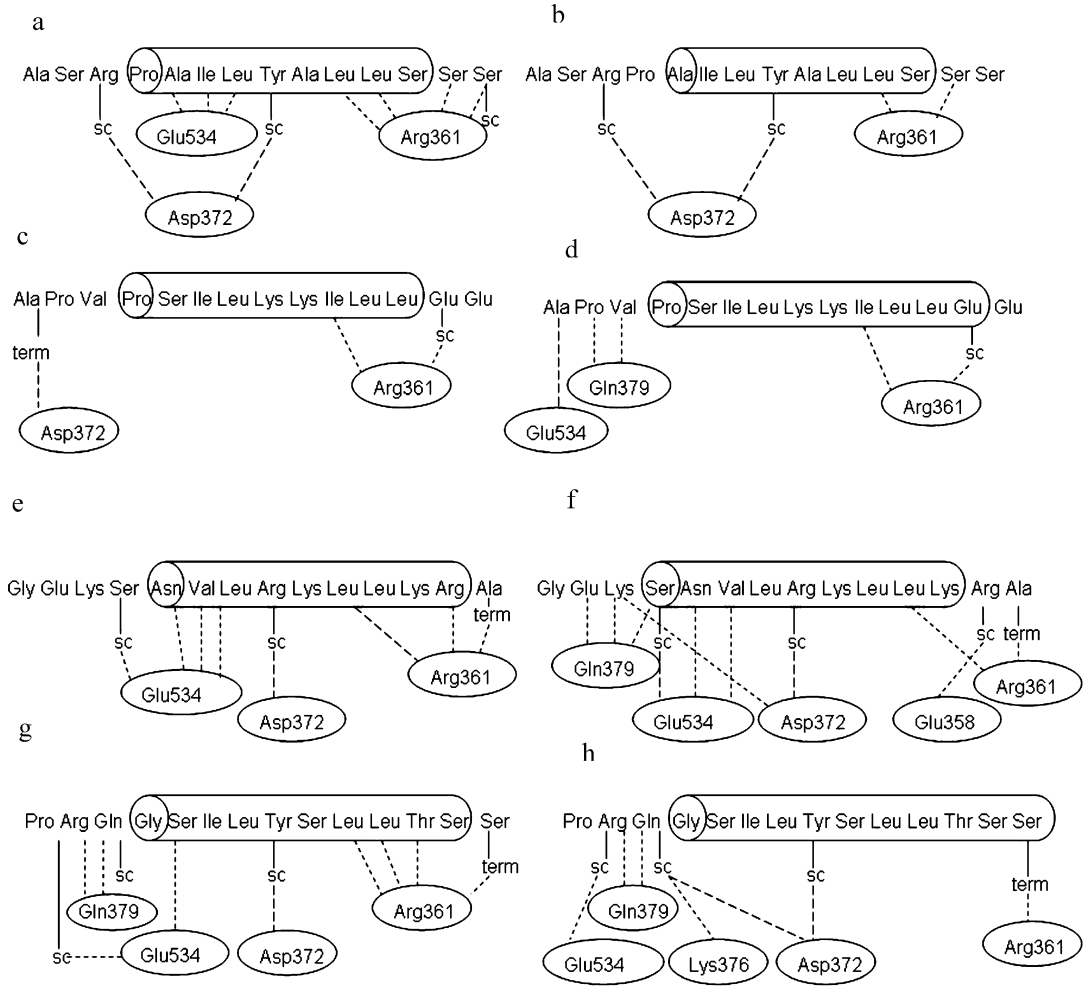

FIGURE 3: Hydrogen bond contact map of the cofactor peptides and the LRH-1 receptor: (a) SHP box1; (b) SHP box1-ps, ligand present; (c) SHP box2; (d) SHP box2-ps, ligand present; (e) PROX1; (f) PROX1-ps, ligand present; (g) DAX-1; (h) DAX-1-ps, ligand present.

important interaction site to lock the peptide −3 position and stabilizing the +2 position (*9*). In our simulations, Met375 is within van der Waals distance to the ligand and contributes to the shape of the cofactor peptide binding site, but more important for residue +2 stabilization is the adjacent and charged Asp372, which often interacts with residues −3/−4 and the side chain of +2. The interaction with Asp372 was also observed in the X-ray structure model of mLRH-1 and SHP box2 (*35*) where it interacts with the peptide +2 residue. Interaction to the peptide +2 site was also suggested together with +6, to form an extra charge-clamp in glucocorticoid receptor and constitutive androstane receptor (*36, 37*). Apart from these studies the Asp372−cofactor peptide interaction is not extensively discussed in the literature. We therefore performed a structural comparison of available X-ray structures in the Protein Data Bank (*25*) of each nuclear receptor type in agonist conformation with a cofactor peptide binding the AF-2 site, and the results reveal an interesting pattern. Apparently the interaction at peptide +2 site can contribute to the stability of the receptor−peptide interaction for several receptors. Hydrogen bonds between an aspartate located in the same position as hLRH-1 Asp372 could likely be formed to the peptide +2 site in RXRα and *β* (*38, 39*), AR (*40*), VDR (*41*) and HNF4α (*42*). The same interaction but with another receptor amino acid could be formed in LXRα and *β* (*39, 43*), ERα (*44*), TR (*45*), FXR (*46*), PPARα and *γ* (*47, 48*). However, the possibility of hydrogen bond formation may depend on the peptide sequence. As seen in the hLRH-1 simulations SHP box1, DAX-3 and PROX1 can form interaction to Asp372, but not SHP box2. The distances between Asp372 and the peptide +2 site range from 2.7 Å in SHP box1 to 11.6 Å in SHP box2, which reflects that large distances can be bridged by side chain movement (Figure 5). We therefore predict that other receptors also can adopt a conformation where the cofactor peptide +2 site can be hydrogen bonded. This can be exemplified with mLRH-1, which shows a distance of 9.4 Å between Asp391 and the +2 site of the SHP box1 peptide, but has been reported to form a hydrogen bond to this site in complex with SHP box2. In the close homologue SF-1 the Asp-site is located on the opposite side of helix 4 compared to the cofactor binding site, and hydrogen binding to this site is unlikely (Figure 5f). The second charge clamp interaction to the peptide +6 residue could not be observed in any of the investigated structures. Frequently either the +6 receptor interaction partner was absent in this location or the receptor side chain orientation pointed away from the +6 site. The X-ray structure of the peptides often shows a +6 side chain orientation out from the receptor. In a full length folded cofactor, the orientation of the +6 residue may differ and allow other interactions, but according to the comparison of receptor−peptide X-ray structures the +6 interaction is of minor importance for the interaction stability. Based on these structural comparisons, data from the

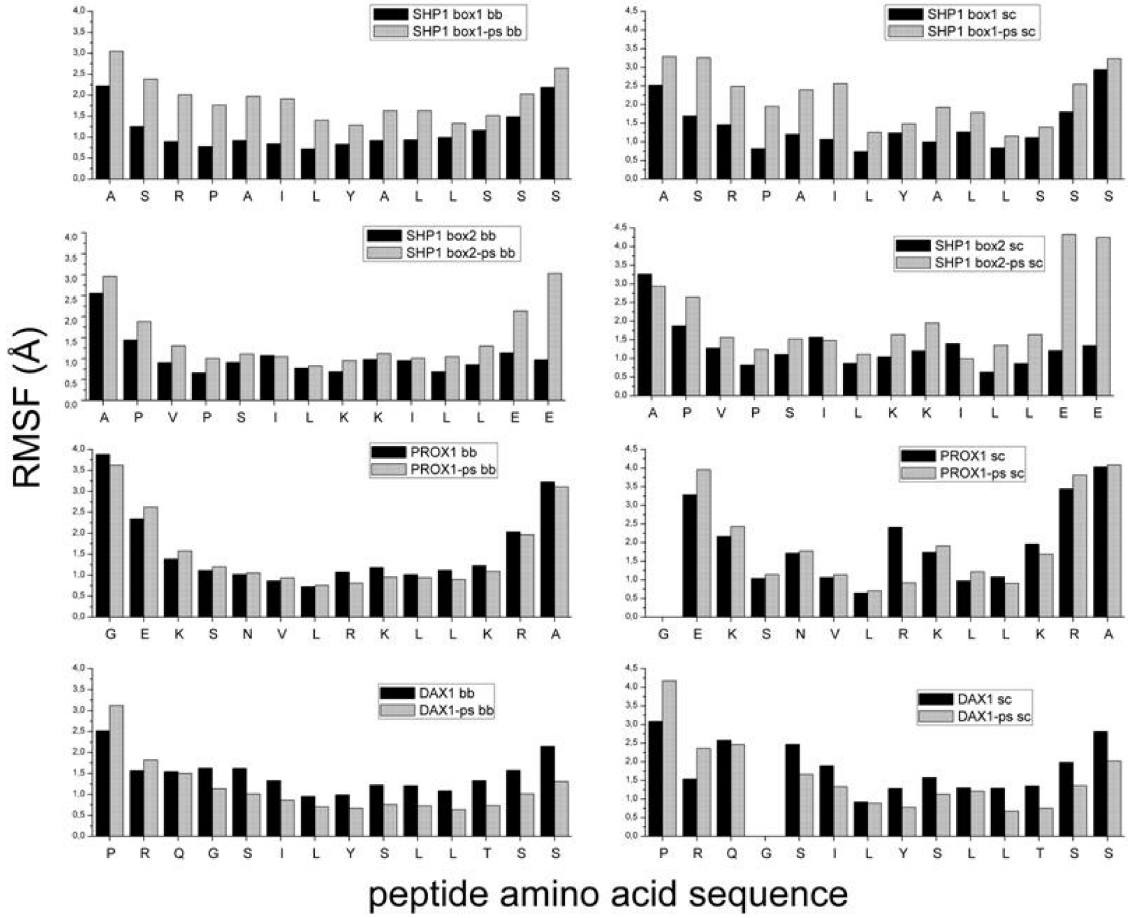

FIGURE 4: rmsf values of the cofactor peptides backbone (bb) and side chain (sc).

Table 3: PS Ligand Hydrogen Bond Interactions[a]

simulation	receptor residue (ligand atom)
SHP box1-ps	Thr341(OT), Tyr516(O6/O7/OG), Lys520(O7/O8/OG)
SHP box2-ps	Gln419(HT), Gly421(OT), Ala422(OT), Tyr516(OG), Lys520(O7)
DAX-1-ps	Lys338(OT), Ser340(O6), Thr341(O4), Phe342(O3), Gln419(O6)
PROX1-ps	Gly421(O7), Tyr516(O6), Lys520(O8,OG), Asp528(HT)

[a] For each simulation the hydrogen bonding receptor residue is given with its interaction partner atom within parenthesis. An OT/HT atom corresponds to atoms on the serine head ends, the OG atom is the oxygen at the serine sidechain. The O5−O8 atoms are found in the phosphate group and O3 atoms on one of the carboxyl oxygens close to the fatty acid tail.

Table 4: Accessible Surface Area (ASA) for LRH-1 h2 and Radius of Gyration (RGYR) of LRH-1[a]

simulation	ASA ± SD (Å^2)	RGYR ± SD (Å)
SHP box1	2118 ± 62	18.5 ± 0.1
SHP box1-ps	2044 ± 57	18.6 ± 0.1
SHP box2	2154 ± 39	18.7 ± 0.1
SHP box2-ps	2123 ± 44	18.6 ± 0.1
DAX-1	2098 ± 48	18.5 ± 0.1
DAX-1-ps	181 ± 74	18.6 ± 0.1
PROX1	2102 ± 38	18.8 ± 0.1
PROX1-ps	2105 ± 45	18.6 ± 0.1

[a] Simulation averages with standard deviations in parentheses.

literature and the results from our simulations, Asp372 site is suggested to play an important role for the molecular recognition of cofactors by hLRH-1 and possibly other NRs. Evidently, the hLRH-1 uses residue Asp372 to extend the two-site charge-clamp to a three-site triangle shaped charge-clamp (Figure 6).

Residues of the peptide involved in specific interaction were also identified. At the peptide N-terminal part, residues from −5 to −3 (counting from the LXXLL motif) are observed as hydrogen bond partners. SHP box1 and DAX-1 show a preference for a −4 hydrogen bond while PROX1 shows hydrogen bond at −3 although the −4 position contains a positively charged amino acid as SHP box1 and DAX-1. The peptides of SHP box1, DAX-1 and PROX1 also show a strong and specific interaction at the +2 position. The +2 interaction is not observed in the SHP box2 simulations even though the position holds a positively charged amino acid. This can be due to the relatively low free energy gain of such a saltbridge formation (*49*). Surprisingly, the SHP box2 simulations form a specific interaction at the +7 position. To conclude, SHP box1, DAX-1 and PROX1 show a similar pattern with specific interactions at −3 or −4 and +2, while SHP box2 only binds specifically at the +7 site.

The terminal interactions (labeled "tm" in Table 2) are not included in the peptide binding discussion since these interactions is a result of an artificial modeling setup (see Methods). However, it is possible that in the simulation these terminal atoms compete with other hydrogen bonding atoms, such as the backbone atoms NH and O. This would cause an underestimation of the number hydrogen bonds and the occupancy at the terminal residues, although some of these terminal hydrogen bond interactions might in reality be replaced by a backbone interaction at that site.

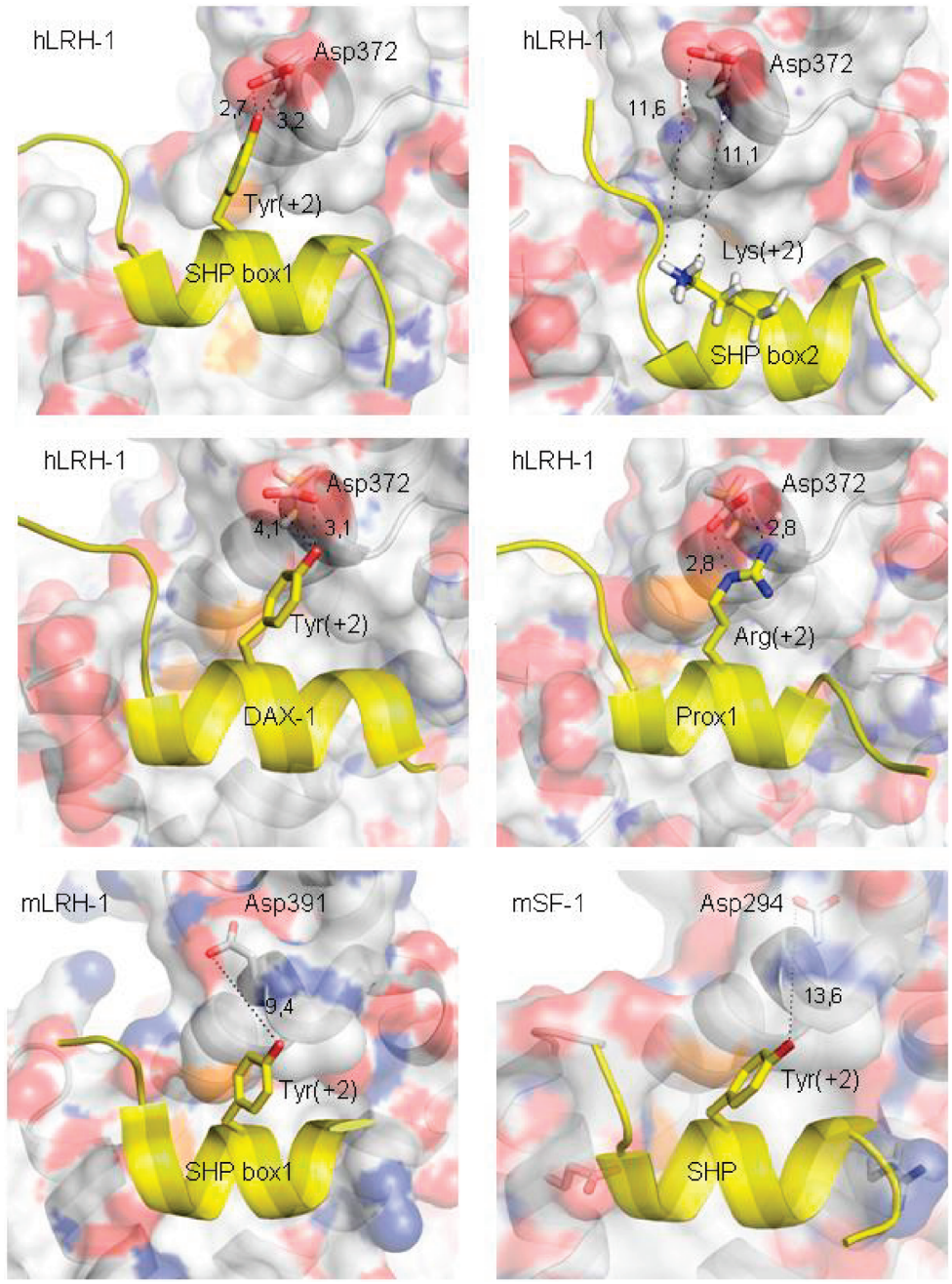

FIGURE 5: Interaction of cofactor peptide +2 site and receptor Asp-site. Plausible interactions are shown with dashed lines, and distances are given in angstroms (Å) The selected representation of hLRH-1 is snapshots from simulations, and mLRH-1 (*10*) and mSF-1 (*12*) show X-ray structures. The receptor surface is colored red for oxygen and blue for nitrogen, and the peptides are shown in yellow cartoons with the +2 site shown in sticks.

Ligand Binding. Ligand−protein hydrogen bond interactions are observed in the regions where the ligand head moves. The SHP box1-ps, SHP box2-ps and the PROX1-ps simulations show the ligand phosphate oxygens bound to h11. This was also observed in the X-ray structure where Tyr516, Lys520 and the amide of Gly501 interact with the phosphate oxygen. Even though no stabilization is observed in any of our simulations, the ligand in each complex tends to prefer a certain region. This observation can be a result of intermolecular communication, meaning that a certain peptide sequence might cause a typical ligand conformation, but it can also be due to insufficient molecular dynamics sampling, if this change of conformation is connected with such a high energy barrier that the transition does not occur in the 10 ns simulation.

H2 Packing. Structurally, the conserved N terminal part (h1−h3) is suggested to be responsible for the LRH-1 LBD stability. The extended h2 of LRH-1 forms an additional fourth layer of the LBD canonical fold and further stabilizes the AF-2 region and h12. The X-ray structure of the liganded receptor shows no major change of h2 conformation (*9*) compared to the unliganded (*10*). In our study, we were able to study 10 ns dynamics of 4 different receptor complexes under the influence of a bound ligand. The trajectory analysis of the packing of h2 (ASA in Table 4) shows no evidence that h2 is affected by the binding of a ligand. Neither does

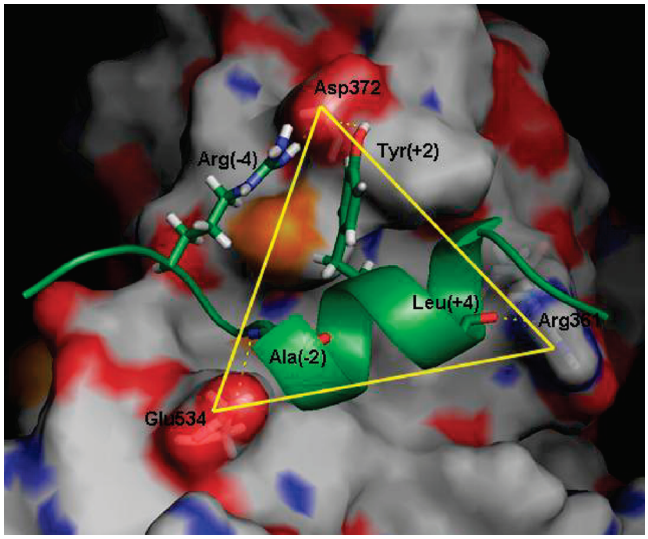

FIGURE 6: Interaction of hLRH-1 and SHP box1. Snapshot from simulation, showing LRH-1 surface colored red for oxygen, blue for nitrogen, orange for sulfur and gray for carbon. The SHP box1 peptide is shown in green cartoon manner. The charge-clamp residues Arg361 and Glu534 together with the additional interaction from Asp372 and its peptide interaction partners are shown in sticks. Together these LRH-1 residues forms a triangle shaped charge-clamp, indicated by yellow lines.

the analysis of the receptor radius of gyration reveal any changes due to the introduction of a ligand (Table 4). Our results confirm the X-ray structure data and verify that the packing of h2 and LRH-1 is not affected by binding of a ligand.

Cofactor Peptide−Receptor Interaction and Ligand Binding. The cofactor peptide−receptor interaction responds differently upon ligand binding according to our simulations. The SHP box1 and box2 simulations show a decrease in total and specific hydrogen bond occupancy (Table 2). The rmsf of the SHP box1 and 2 peptide backbone and side chains also reveal a more flexible peptide when bound to ligand (Figure 4). This indicates that upon ligand binding the hLRH-1 interactions with SHP box1 and box2 peptides are weakened. The DAX-1 peptide shows a decrease in hydrogen bonds and occupancy, but an increase in specific binding and no change in specific occupancy. The decrease of the total occupancy is highly affected by the Arg361 interaction. In DAX-1 the Arg361 binds the backbone of the peptide C-terminal part, whereas in the DAX-1-ps the Arg361 is oriented toward the C-terminal atoms not included in the occupancy summation. In a full length DAX-1 cofactor it is probable that the Arg361 interaction present in the DAX-1 simulation would be repeated for DAX-1-ps. The peptide becomes less flexible upon ligand binding according to the rmsf calculations. Thus the interaction between the DAX-1 cofactor peptide and hLRH-1 is likely strengthened upon ligand binding. The PROX1 interactions and specific occupancy are increased upon ligand binding. The rmsf calculations also show a stable peptide when ligand bound. Notable is the drop of rmsf in the PROX1-ps +2 site. This site holds the Tyr (+2) which is involved in a specific hydrogen bond. Tyr (+2) hydrogen bond occupancy increases from 40% to 98% and the average hydrogen bond time (Table 2) increases from 70 to 612 ps, when a ligand is introduced, which explains the difference in side chain fluctuations. Thus, a bound ligand seems to strengthen the hLRH-1 interaction with peptide PROX1.

Orphan Receptors and Ligands. Why is it so important to find ligands for orphan receptors? Experimental data actually suggest that the hLRH-1 is truly ligand independent (*14*). The constitutively active conformation found with X-ray where the ligand binding pocket is empty indicates that no natural ligand is needed. Additionally, mutational studies introducing bulky side chains into the LBP do not affect LRH-1 activity (*10*). These findings have led to the conclusion that ligands are not important for the basal activity. However, ligand binding cannot be totally excluded. The constitutively active conformation of hLRH-1 with an empty ligand binding pocket triggers the idea to reach a "superactive" LRH-1 conformation. This could be achieved by the binding of a ligand. Steps in this direction have recently been made, when a small ligand was found to bind LRH-1 (*50*) and increase its activity. Phospholipids as ligands are not suitable lead targets for the pharmaceutical industry, but binding of these ligands might provide information of the receptor's biological activity. X-ray studies show evidence that a phospholipid can bind to the receptor, and biochemical studies reveal that the dissociation from the receptor is on the same time scale as receptor degradation. Therefore it is not likely that the hLRH-1 phospholipid ligands serve as regulatory on−off switches as seen in steroid nuclear receptors. However, our results show that even though the hLRH-1 receptor structure is rather unaffected by the binding of a ligand, the interactions with the cofactors change upon ligand binding. Also, the different cofactor peptides respond differently to ligand binding. Therefore the regulatory effect of a phospholipid ligand bound to hLRH-1 could be in its modification of cofactor interactions. Based on the resemblance of the molecular recognition of coactivators and corepressors of hLRH-1, it is therefore likely that also coactivators would be affected by ligand binding.

Interactions with peroxisome proliferator-activated receptor γ coactivator-1α (PGC-1α) have been investigated, and PGC-1α was shown to interact with LRH-1 in human breast preadipocytes but not in other tissues of postmenopausal women (*51*). Disruption of the PGC-1α-hLRH-1 interaction would inhibit aromatase activity in breast and thus create a target for development of a more specific antiestrogen therapy for breast cancer. It would therefore be of exceptional interest to see how binding of a ligand would affect the interaction between PGC-1α-hLRH-1. Given the diversity and importance of the possible LRH-1 targets it is encouraging to see the progress made in the work with SF-1, where an inverse agonist was found to repress activity (*52*). The same compound was also tested on LRH-1 without effects, indicating that a natural ligand might be able to distinguish between SF-1 and LRH-1.

CONCLUSION

MD simulations of hLRH-1 and the cofactor peptides SHP box1 and box2, DAX-1 and PROX1 were performed in the presence of a human phospholipid ligand. All our simulations show a stable receptor conformation, both with an empty ligand binding pocket and with a ligand bound over a 10 ns time scale. The packing of the receptor and its interaction with h2 is unchanged in all our simulations. We conclude

that the receptor can maintain the agonist conformation with the PS ligand and the cofactors bound to it.

The receptor−peptide interactions respond differently to the binding of a ligand. The SHP box1 and SHP box 2 peptides reduce their interaction with hLRH-1 upon ligand binding while DAX-1 and PROX1 peptides maintain or increase LRH-1 interaction. The peptides also exhibit different specific binding patterns. SHP box1, PROX1 and DAX-1 form specific hydrogen bonds at −4 or −3 and +2 site while SHP box2 only binds specific at the +7 site. The receptor orients the cofactor peptides with the charge clamp residues Arg361 and Glu 534. Additionally Asp372 was frequently seen to form specific hydrogen bonds to the cofactor peptide +2 site. A structural comparison of NRs in agonist conformation with a cofactor peptide bound to it revealed that the Asp-site might form hydrogen bonds in several receptor types upon given cofactor binding. We suggest that the Asp-site is important for cofactor peptide binding and forms a third corner in a triangle shaped charge clamp. The results obtained imply that ligand binding can be used to modify the cofactor−receptor binding. This gives an opportunity to design drugs which can in a very specific way interact with a cofactor−receptor complex and affect transcription.

REFERENCES

1. Mangelsdorf, D. J., Thummel, C., Beato, M., Herrlich, P., Schutz, G., Umesono, K., Blumberg, B., Kastner, P., Mark, M., Chambon, P., and Evans, R. M. (1995) The nuclear receptor superfamily: the second decade. *Cell 83*, 835–839.
2. Mangelsdorf, D. J., Ong, E. S., Dyck, J. A., and Evans, R. M. (1990) Nuclear receptor that identifies a novel retinoic acid response pathway. *Nature 345*, 224–229.
3. Nuclear Receptors Nomenclature Committee. (1999) A unified nomenclature system for the nuclear receptor superfamily. *Cell 97*, 161−163.
4. Mataki, C., Magnier, B. C., Houten, S. M., Annicotte, J. S., Argmann, C., Thomas, C., Overmars, H., Kulik, W., Metzger, D., Auwerx, J., and Schoonjans, K. (2007) Compromised intestinal lipid absorption in mice with a liver-specific deficiency of liver receptor homolog 1. *Mol. Cell. Biol. 27*, 8330–8339.
5. Sanyal, S., Bavner, A., Haroniti, A., Nilsson, L. M., Lundasen, T., Rehnmark, S., Witt, M. R., Einarsson, C., Talianidis, I., Gustafsson, J. A., and Treuter, E. (2007) Involvement of corepressor complex subunit GPS2 in transcriptional pathways governing human bile acid biosynthesis. *Proc. Natl. Acad. Sc.i U.S.A. 104*, 15665–15670.
6. Zhou, Q., Chipperfield, H., Melton, D. A., and Wong, W. H. (2007) A gene regulatory network in mouse embryonic stem cells. *Proc. Natl. Acad. Sci. U.S.A. 104*, 16438–16443.
7. Benoit, G., Malewicz, M., and Perlmann, T. (2004) Digging deep into the pockets of orphan nuclear receptors: insights from structural studies. *Trends Cell Biol. 14*, 369–376.
8. Rosenfeld, M. G., Lunyak, V. V., and Glass, C. K. (2006) Sensors and signals: a coactivator/corepressor/epigenetic code for integrating signal-dependent programs of transcriptional response. *Genes Dev. 20*, 1405–1428.
9. Ortlund, E. A., Lee, Y., Solomon, I. H., Hager, J. M., Safi, R., Choi, Y., Guan, Z., Tripathy, A., Raetz, C. R., McDonnell, D. P., Moore, D. D., and Redinbo, M. R. (2005) Modulation of human nuclear receptor LRH-1 activity by phospholipids and SHP. *Nat. Struct. Mol. Biol. 12*, 357–363.
10. Sablin, E. P., Krylova, I. N., Fletterick, R. J., and Ingraham, H. A. (2003) Structural basis for ligand-independent activation of the orphan nuclear receptor LRH-1. *Mol. Cell 11*, 1575–1585.
11. Krylova, I. N., Sablin, E. P., Moore, J., Xu, R. X., Waitt, G. M., MacKay, J. A., Juzumiene, D., Bynum, J. M., Madauss, K., Montana, V., Lebedeva, L., Suzawa, M., Williams, J. D., Williams, S. P., Guy, R. K., Thornton, J. W., Fletterick, R. J., Willson, T. M., and Ingraham, H. A. (2005) Structural analyses reveal phosphatidyl inositols as ligands for the NR5 orphan receptors SF-1 and LRH-1. *Cell 120*, 343–355.
12. Li, Y., Choi, M., Cavey, G., Daugherty, J., Suino, K., Kovach, A., Bingham, N. C., Kliewer, S. A., and Xu, H. E. (2005) Crystallographic identification and functional characterization of phospholipids as ligands for the orphan nuclear receptor steroidogenic factor-1. *Mol. Cell 17*, 491–502.
13. Forman, B. M. (2005) Are those phospholipids in your pocket. *Cell Metab. 1*, 153–155.
14. Fayard, E., Auwerx, J., and Schoonjans, K. (2004) LRH-1: an orphan nuclear receptor involved in development, metabolism and steroidogenesis. *Trends Cell Biol. 14*, 250–260.
15. Heery, D. M., Kalkhoven, E., Hoare, S., and Parker, M. G. (1997) A signature motif in transcriptional co-activators mediates binding to nuclear receptors. *Nature 387*, 733–736.
16. Nolte, R. T., Wisely, G. B., Westin, S., Cobb, J. E., Lambert, M. H., Kurokawa, R., Rosenfeld, M. G., Willson, T. M., Glass, C. K., and Milburn, M. V. (1998) Ligand binding and co-activator assembly of the peroxisome proliferator-activated receptor-gamma. *Nature 395*, 137–143.
17. Nagy, L., Kao, H. Y., Love, J. D., Li, C., Banayo, E., Gooch, J. T., Krishna, V., Chatterjee, K., Evans, R. M., and Schwabe, J. W. (1999) Mechanism of corepressor binding and release from nuclear hormone receptors. *Genes Dev. 13*, 3209–3216.
18. McInerney, E. M., Rose, D. W., Flynn, S. E., Westin, S., Mullen, T. M., Krones, A., Inostroza, J., Torchia, J., Nolte, R. T., Assa-Munt, N., Milburn, M. V., Glass, C. K., and Rosenfeld, M. G. (1998) Determinants of coactivator LXXLL motif specificity in nuclear receptor transcriptional activation. *Genes Dev. 12*, 3357–3368.
19. Suzuki, T., Kasahara, M., Yoshioka, H., Morohashi, K., and Umesono, K. (2003) LXXLL-related motifs in Dax-1 have target specificity for the orphan nuclear receptors Ad4BP/SF-1 and LRH-1. *Mol. Cell. Biol. 23*, 238–249.
20. Chang, C., Norris, J. D., Gron, H., Paige, L. A., Hamilton, P. T., Kenan, D. J., Fowlkes, D., and McDonnell, D. P. (1999) Dissection of the LXXLL nuclear receptor-coactivator interaction motif using combinatorial peptide libraries: discovery of peptide antagonists of estrogen receptors alpha and beta. *Mol. Cell. Biol. 19*, 8226–8239.
21. Bavner, A., Sanyal, S., Gustafsson, J. A., and Treuter, E. (2005) Transcriptional corepression by SHP: molecular mechanisms and physiological consequences. *Trends Endocrinol. Metab. 16*, 478–488.
22. Lalli, E., and Sassone-Corsi, P. (2003) DAX-1, an unusual orphan receptor at the crossroads of steroidogenic function and sexual differentiation. *Mol. Endocrinol. 17*, 1445–1453.
23. Steffensen, K. R., Holter, E., Bavner, A., Nilsson, M., Pelto-Huikko, M., Tomarev, S., and Treuter, E. (2004) Functional conservation of interactions between a homeodomain cofactor and a mammalian FTZ-F1 homologue. *EMBO Rep. 5*, 613–619.
24. Qin, J., Gao, D. M., Jiang, Q. F., Zhou, Q., Kong, Y. Y., Wang, Y., and Xie, Y. H. (2004) Prospero-related homeobox (Prox1) is a corepressor of human liver receptor homolog-1 and suppresses the transcription of the cholesterol 7-alpha-hydroxylase gene. *Mol. Endocrinol. 18*, 2424–2439.
25. Bernstein, F. C., Koetzle, T. F., Williams, G. J., Meyer, E. F., Jr., Brice, M. D., Rodgers, J. R., Kennard, O., Shimanouchi, T., and Tasumi, M. (1977) The Protein Data Bank: a computer-based archival file for macromolecular structures. *J. Mol. Biol. 112*, 535–542.
26. MacKerell, A. D., Bashford, D., Bellott, M., Dunbrack, R. L., Evanseck, J. D., Field, M. J., Fischer, S., Gao, J., Guo, H., Ha, S., Joseph-McCarthy, D., Kuchnir, L., Kuczera, K., Lau, F. T. K., Mattos, C., Michnick, S., Ngo, T., Nguyen, D. T., Prodhom, B., Reiher, W. E., Roux, B., Schlenkrich, M., Smith, J. C., Stote, R., Straub, J., Watanabe, M., Wiorkiewicz-Kuczera, J., Yin, D., and Karplus, M. (1998) All-Atom Empirical Potential for Molecular Modeling and Dynamics Studies of Proteins. *J. Phys. Chem. B 102*, 3586–3616.
27. Brunger, A. T., and Karplus, M. (1988) Polar hydrogen positions in proteins: empirical energy placement and neutron diffraction comparison. *Proteins 4*, 148–56.
28. Brooks, B. R., Bruccoleri, R. E., Olafson, B. D., States, D. J., Swaminathan, S., and Karplus, M. (1983) CHARMM: a program for macromolecular energy, minimization, and dynamics calculations. *J. Comput. Chem. 4*, 187–217.

29. Jorgensen, W. L., Chandrasekhar, J., Madura, J. D., Impey, R. W., and Klein, M. L. (1983) Comparison of simple potential functions for simulating liquid water. *J. Chem. Phys. 79*, 926–935.
30. Ryckaert, J. P., Ciccotti, G., and Berendsen, H. J. C. (1977) Numerical integration of the cartesian equations of motion of a system with constraints: Molecular dynamics of n-alkanes. *J. Comput. Chem.* 327–341.
31. De Loof, H., Nilsson, L., and Rigler, R. (1992) Molecular dynamics simulation of galanin in aqueous and nonaqueous solution. *J. Am. Chem. Soc. 114*, 4028–4035.
32. Lee, B., and Richards, F. M. (1971) The interpretation of protein structures: estimation of static accessibility. *J. Mol. Biol. 55*, 379–400.
33. Li, Y., Lambert, M. H., and Xu, H. E. (2003) Activation of nuclear receptors: a perspective from structural genomics. *Structure 11*, 741–746.
34. Wagner, R. L., Apriletti, J. W., McGrath, M. E., West, B. L., Baxter, J. D., and Fletterick, R. J. (1995) A structural role for hormone in the thyroid hormone receptor. *Nature 378*, 690–697.
35. Li, Y., Choi, M., Suino, K., Kovach, A., Daugherty, J., Kliewer, S. A., and Xu, H. E. (2005) Structural and biochemical basis for selective repression of the orphan nuclear receptor liver receptor homolog 1 by small heterodimer partner. *Proc. Natl. Acad. Sci. U.S.A. 102*, 9505–9510.
36. Bledsoe, R. K., Montana, V. G., Stanley, T. B., Delves, C. J., Apolito, C. J., McKee, D. D., Consler, T. G., Parks, D. J., Stewart, E. L., Willson, T. M., Lambert, M. H., Moore, J. T., Pearce, K. H., and Xu, H. E. (2002) Crystal structure of the glucocorticoid receptor ligand binding domain reveals a novel mode of receptor dimerization and coactivator recognition. *Cell 110*, 93–105.
37. Suino, K., Peng, L., Reynolds, R., Li, Y., Cha, J. Y., Repa, J. J., Kliewer, S. A., and Xu, H. E. (2004) The nuclear xenobiotic receptor CAR: structural determinants of constitutive activation and heterodimerization. *Mol. Cell 16*, 893–905.
38. Egea, P. F., Mitschler, A., and Moras, D. (2002) Molecular recognition of agonist ligands by RXRs. *Mol. Endocrinol. 16*, 987–997.
39. Svensson, S., Ostberg, T., Jacobsson, M., Norstrom, C., Stefansson, K., Hallen, D., Johansson, I. C., Zachrisson, K., Ogg, D., and Jendeberg, L. (2003) Crystal structure of the heterodimeric complex of LXRalpha and RXRbeta ligand-binding domains in a fully agonistic conformation. *EMBO J. 22*, 4625–4633.
40. Estebanez-Perpina, E., Moore, J. M., Mar, E., Delgado-Rodrigues, E., Nguyen, P., Baxter, J. D., Buehrer, B. M., Webb, P., Fletterick, R. J., and Guy, R. K. (2005) The molecular mechanisms of coactivator utilization in ligand-dependent transactivation by the androgen receptor. *J. Biol. Chem. 280*, 8060–8068.
41. Vanhooke, J. L., Benning, M. M., Bauer, C. B., Pike, J. W., and DeLuca, H. F. (2004) Molecular structure of the rat vitamin D receptor ligand binding domain complexed with 2-carbon-substituted vitamin D3 hormone analogues and a LXXLL-containing coactivator peptide. *Biochemistry 43*, 4101–4110.
42. Duda, K., Chi, Y. I., and Shoelson, S. E. (2004) Structural basis for HNF-4alpha activation by ligand and coactivator binding. *J. Biol. Chem. 279*, 23311–23316.
43. Williams, S., Bledsoe, R. K., Collins, J. L., Boggs, S., Lambert, M. H., Miller, A. B., Moore, J., McKee, D. D., Moore, L., Nichols, J., Parks, D., Watson, M., Wisely, B., and Willson, T. M. (2003) X-ray crystal structure of the liver X receptor beta ligand binding domain: regulation by a histidine-tryptophan switch. *J. Biol. Chem. 278*, 27138–27143.
44. Warnmark, A., Treuter, E., Gustafsson, J. A., Hubbard, R. E., Brzozowski, A. M., and Pike, A. C. (2002) Interaction of transcriptional intermediary factor 2 nuclear receptor box peptides with the coactivator binding site of estrogen receptor alpha. *J. Biol. Chem. 277*, 21862–21868.
45. Darimont, B. D., Wagner, R. L., Apriletti, J. W., Stallcup, M. R., Kushner, P. J., Baxter, J. D., Fletterick, R. J., and Yamamoto, K. R. (1998) Structure and specificity of nuclear receptor-coactivator interactions. *Genes Dev. 12*, 3343–3356.
46. Mi, L. Z., Devarakonda, S., Harp, J. M., Han, Q., Pellicciari, R., Willson, T. M., Khorasanizadeh, S., and Rastinejad, F. (2003) Structural basis for bile acid binding and activation of the nuclear receptor FXR. *Mol. Cell 11*, 1093–1100.
47. Xu, H. E., Lambert, M. H., Montana, V. G., Plunket, K. D., Moore, L. B., Collins, J. L., Oplinger, J. A., Kliewer, S. A., Gampe, R. T., Jr., McKee, D. D., Moore, J. T., and Willson, T. M. (2001) Structural determinants of ligand binding selectivity between the peroxisome proliferator-activated receptors. *Proc. Natl. Acad. Sci. U.S.A. 98*, 13919–13924.
48. Burgermeister, E., Schnoebelen, A., Flament, A., Benz, J., Stihle, M., Gsell, B., Rufer, A., Ruf, A., Kuhn, B., Marki, H. P., Mizrahi, J., Sebokova, E., Niesor, E., and Meyer, M. (2006) A novel partial agonist of peroxisome proliferator-activated receptor-gamma (PPARgamma) recruits PPARgamma-coactivator-1alpha, prevents triglyceride accumulation, and potentiates insulin signaling in vitro. *Mol. Endocrinol. 20*, 809–830.
49. Kumar, S., and Nussinov, R. (2001) Fluctuations in ion pairs and their stabilities in proteins. *Proteins 43*, 433–454.
50. Whitby, R. J., Dixon, S., Maloney, P. R., Delerive, P., Goodwin, B. J., Parks, D. J., and Willson, T. M. (2006) Identification of small molecule agonists of the orphan nuclear receptors liver receptor homolog-1 and steroidogenic factor-1. *J. Med. Chem. 49*, 6652–6655.
51. Safi, R., Kovacic, A., Gaillard, S., Murata, Y., Simpson, E. R., McDonnell, D. P., and Clyne, C. D. (2005) Coactivation of liver receptor homologue-1 by peroxisome proliferator-activated receptor gamma coactivator-1alpha on aromatase promoter II and its inhibition by activated retinoid X receptor suggest a novel target for breast-specific antiestrogen therapy. *Cancer Res. 65*, 11762–11770.
52. Del Tredici, A. L., Andersen, C. B., Currier, E. A., Ohrmund, S. R., Fairbain, L. C., Lund, B. W., Nash, N., Olsson, R., and Piu, F. (2008) Identification of the first synthetic steroidogenic factor 1 inverse agonists: pharmacological modulation of steroidogenic enzymes. *Mol. Pharmacol. 73*, 900–908.

BI7025084